J. Plasma Physics (2010), *vol.* 76, *parts* 3&4, *pp.* 467–476.
doi:10.1017/S0022377809990699

Stable localized electromagnetic pulses in asymmetric pair plasmas

V. I. BEREZHIANI[1,2],
S.M. MAHAJAN[3] and N.L. SHATASHVILI[1,2]

[1] Plasma Physics Department, Andronikashvili Institute of Physics, Tbilisi 0177, Georgia (shatashvili@yahoo.com)

[2] Department of Physics, Faculty of Exact and Natural Sciences, Javakhishvili Tbilisi State University, Tbilisi 0128, Georgia

[3] Institute for Fusion Studies, The University of Texas at Austin, Austin,Tx 78712, USA

(Received 28 November 2009 and accepted 9 December 2009, first published online 15 January 2010)

Abstract. It is shown that pair plasmas, through the new focusing–defocusing nonlinearity generated by an 'asymmetry' in initial temperatures of constituent species, can support multidimensional, stable, large-amplitude light bullets as well as bullets carrying vortices, *i.e.* spinning bullets.

1. Model

The pair plasmas consisting of only positive- and negative-charged particles of equal mass have attracted special attention mainly because of astrophysical applications. In the early Universe during the lepton era, ultra-relativistic electron–positron (e–p) pairs contributed dominantly to the matter content of the Universe [1]. The gamma-ray bursts – the most concentrated electromagnetic explosions in the Universe – are believed to be related with the enormous energy release in compact regions in short time scales. This energy release leads to the formation of a highly dense optically thick e–p plasma that expands and cools while remaining relativistic [2]. Such pair plasmas also exist in active galactic nuclei, in the relativistic jets [3] and in the pulsar magnetospheres [4].

Properties of pair plasmas are different from ordinary electron–ion plasma. It is important to investigate the dynamics of such plasmas in the laboratory conditions not only from the point of view of fundamental physics but also to reproduce the dynamical phenomena taking place in astrophysical environments. Ultrastrong laser pulses are another source for intense pair-creation in laboratory conditions [5]. The story of laboratory pair plasmas had its defining moment with the successful creation of a 'sufficiently' dense pair-ion (pi) plasma – consisting of equal-mass, positive and negative fullerene (C_{60}^{+} and C_{60}^{-}) [6] or hydrogen (H^{+}– H^{-}) ions [7, 8]. Unlike the e–p plasma systems (both of the astrophysical and laboratory variety), such pair of ion plasmas have long enough life time so that the collective behavior peculiar to the plasma state can be experimentally investigated under controlled conditions.

The theoretical research in the electromagnetic properties of symmetric pair plasmas has a long and rich history [9]. Somewhat different class of phenomena

is made possible when the pi plasmas are not fully symmetric; this could happen when the pair plasma is contaminated by free electrons or by a fraction of ions of different mass [10]. Different species may not be produced in identical conditions [11]. For instance, the positive and negative ions could have different thermal speeds (temperatures).

The present study concentrates on establishing the existence of 3-dimensional (3D), fully localized electromagnetic (EM) structures – 'light bullets' – in asymmetric pair plasmas; mathematical formulation turns out to be quite similar for asymmetries of different origin. It was shown in a recent study [12] that when asymmetries originate in small temperature differences in the constituent species, the dynamics of EM pulses can be described by the following Nonlinear Schrödinger Equation (NLS):

$$2i\omega_0 \frac{\partial A}{\partial t} + \frac{(2-\epsilon)}{\omega_0^2} \frac{\partial^2 A}{\partial Z^2} + \nabla_\perp^2 A + F(|A|^2) \cdot A = 0. \tag{1.1}$$

Note that this equation, derived in the parabolic approximation, is endowed with a new type of nonlinearity

$$F(|A|^2) = \frac{\epsilon^2}{2} \frac{\kappa |A|^2}{(1+\kappa |A|^2)^2}. \tag{1.2}$$

Following assumptions and definitions have gone into the derivation of (1.1) and (1.2) in perspective: A is the slowly varying amplitude of the circularly polarized EM pulse $\sim A(\hat{\mathbf{x}} + \hat{\mathbf{y}}) \exp(\mathrm{i}k_0 \mathrm{z} - \omega_0 \mathrm{t})$ with mean frequency ω_0 and mean wave number k_0; $\nabla_\perp^2 = \partial^2/\partial x^2 + \partial^2/\partial y^2$ is the diffraction operator and $Z = z - v_g t$ is the 'comoving' (with group velocity v_g) coordinate.

Equation (1.1) is written in terms of the dimensionless quantities $r = (\omega_e/c)r$, $t = \omega_e t$, $A = |e|A/(mG(T_0^-)c^2)$, where $\omega_e = (4\pi e^2 n_0/m)^{1/2}$ is the electron Langmuir frequency and m is the electron mass. The charges $q^\pm$ and masses $m^\pm$ of positive and negative ions are assumed to be same (in this paper we mainly concentrate on the specific case of pair plasma consisting of electrons and positrons, *i.e.* $q^+ = e^+ = q^- = -e^- = |e|$ and $m^+ = m^- = m$). The equilibrium state of the system is characterized by an overall charge neutrality $n_0^+ = n_0^- = n_0$, where n_0^+ and n_0^- are the unperturbed number densities of the positive and negative ions respectively. The background temperatures of plasma species are $T_0^\pm$ ($T_0^+ \neq T_0^-$) and $m\,G(z^\pm) = m\,K_3(z^\pm)/K_2(z^\pm)$ is the 'effective mass' [$z^\pm = mc^2/T^\pm$], where K_ν are the modified Bessel functions. For the non-relativistic temperatures ($T^\pm \ll mc^2$) $G^\pm = 1 + 5T^\pm/2mc^2$ and for the ultrarelativistic temperatures ($T^\pm \gg m_\alpha c^2$) $G^\pm = 4T^\pm/mc^2 \gg 1$. The smallness parameter $\epsilon = [G(T_0^+) - G(T_0^-)]/G(T_0^+)$ measures the temperature asymmetry of plasma species for the non-relativistic temperatures $\epsilon = 5(T_0^+ - T_0^-)/2mc^2$, while in ultrarelativistic case $\epsilon = (T_0^+ - T_0^-)/T_0^+$. The numerical factor $\kappa = 1/2$ (2/3) for non-relativistic (ultrarelativistic) temperatures. In deriving (1.1) with (1.2), we have assumed that the plasma is transparent ($\omega_0 \gg 1$, $v_g \approx 1$), and that the longitudinal extent of the pulse is much shorter than its transverse spread. For a transparent medium ($\omega_0 \gg 1$), despite the ordering, $\partial A/\partial Z \gg \nabla_\perp A$, the second and the third terms in (1.1) can be comparable.

With self-evident renormalization, (1.1) can be written as

$$i\frac{\partial A}{\partial t} + \frac{\partial^2 A}{\partial Z^2} + \nabla_\perp^2 A + f(|A|^2) \cdot A = 0, \tag{1.3}$$

in which the nonlinearity function [12]

$$f(|A|^2) = \frac{|A|^2}{(1+|A|^2)^2} \tag{1.4}$$

has an unusual feature, *i.e.* in the ultrarelativistic limit $(|A|^2 \gg 1)$ it tends to be 0.

Note that the nonlinear refraction index for the considered system can be written as $\delta n_{nl} = f(I)$ in terms of the EM field intensity $I = |A|^2$. It is easy, then, to work out that for low intensities, $I < 1$, the medium is self-focusing $(d(\delta n_{nl})/dI > 0)$, while for higher intensities $(I > 1)$ it turns defocusing $(d(\delta n_{nl})/dI < 0)$. For the localized intense EM pulse with the peak intensity $I_m > 1$, the region near the pulse peak will tend to broaden while the wings will get sharper.

An immediate consequence of the fucusing–defocusing saturating nonlinearity (originating from the temperature asymmetry) can be illustrated by considering a modulation instability of a quasi-monochromatic EM wave. Equation (1.3) is satisfied by the plane wave solution $A = A_0 \exp(i\tau F(|A_0|^2)) + c.c.$ The standard stability analysis then shows that a linear modulation with frequency Ω and wave number $\mathbf{K}$ obeys the dispersion relation $\Omega^2 = \mathbf{K}^2[\mathbf{K}^2 - 2A_0^2(1-A_0^2)/(1+A_0^2)^3]$, which exhibits a purely growing mode if $A_0 < 1$ and $K < K_{cr} = \sqrt{2A_0^2(1-A_0^2)/(1+A_0^2)^3}$, while for the ultrarelativistic case $(A_0 > 1)$ there is no modulation instability. One can expect that the modulation instability of moderately intense field $(A_0 < 1)$ in the nonlinear stage will lead to the break up of the field into soliton-like pulses with a characteristic length corresponding to the optimum scale of instability $(\sim \sqrt{2}/K_{cr})$.

2. Light bullets in pair plasmas

In what follows, we investigate the possibility of finding stable solitonic solutions of (1.3). For stationary solitons, we look for solutions that are 'spherically' symmetric: $A = A(r)\exp(i\lambda)$, where λ is a constant measuring the nonlinear frequency shift. Notice that the comoving coordinate (Z) can be treated on an equal footing with the spatial coordinate ($\mathbf{r}_\perp$). In terms of the radial variable $r = \left(\mathbf{r}_\perp^2 + Z^2\right)^{1/2}$, (1.3) reduces to an ordinary differential equation that can not be analytically solved:

$$\frac{d^2A}{dr^2} + \frac{2}{r}\frac{dA}{dr} - \lambda A + \frac{A^3}{(1+A^2)^2} = 0. \tag{2.1}$$

It is possible to map this equation in the (A, A_r) plane (phase plane) and show that it admits localized solutions. It can exist in the form of an infinite number of discrete bound states $A_n(r)$ $(n = 0, 1, 2, ...)$, where the radial quantum number n denotes the finite r zeros of the Eigenfunction.

We have numerically solved the Eigenvalue problem of (1.3) for its fundamental solitary solution $(n = 0)$. The calculated dispersion relation is displayed in Fig. 1. One can see that the localized solution exists in the range $0 < \lambda < 0.193$, while the soliton amplitude (A_m) is bounded from above, $A_m < 1.68$. The vanishing saturating nonlinearity, thus, does not sustain solitonic solutions with ultra-relativistic amplitudes $(A_m \gg 1)$ in stark contrast to the ordinary saturating nonlinearity. Another consequences of the vanishing focusing–defocusing nonlinearity is evident in Fig. 2, where the profiles of stationary solutions for different λs are exhibited; one can see that when pulse amplitude approaches the critical value the profile acquires a flat-top.

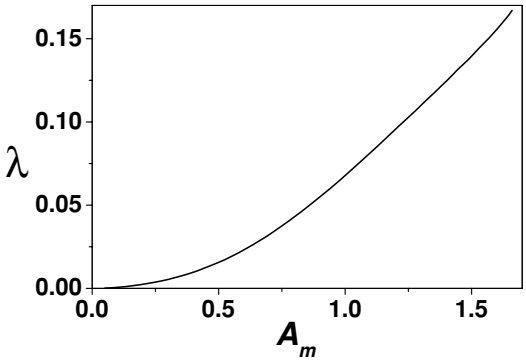

Figure 1. Nonlinear dispersion relation: the effective Eigenvalue λ as a function of A_m .

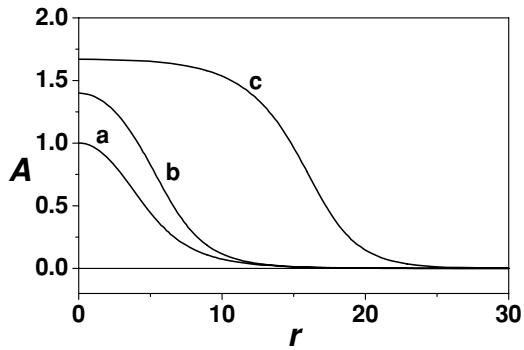

Figure 2. Stationary soliton solution for 3D for different critical Eigenvalues. Plot 'a' corresponds to $\lambda = 06774722$ with $A_m = 1$; plot 'b' corresponds to $\lambda = 0.12451945$ with $A_m = 1.4$ and plot 'c' corresponds to $\lambda = 0.19222242$ with $A_m = 1.67$ respectively. Plot 'c' represents the flat-top soliton solution.

The stability of the obtained solutions can be tested by applying the Vakhitov & Kolokolov criterion (see [13] and references therein), according to which the solition is stable if $\partial N/\partial\lambda > 0$, where $N = \int d\mathbf{r}_\perp dZ\, |A|^2$ is the soliton energy ('photon number'). Because A_m is a growing function of λ, $\partial N/\partial A_m > 0$ insures $\partial N/\partial\lambda > 0$. For 3D solitons of Fig. 3, $\partial N/\partial A_m > 0$ provided $N > N_{cr} = 236.8$ and $A_m > 0.6$. Thus, a soliton with amplitude $A_m > 0.6$ is always stable.

We have used numerical methods to verify the stability of the derived solutions. Direct simulation of (1.3) shows that if an initial profile of the pulse is close to the stable equilibrium (the exact numerical solution), the pulse quickly attains the profile of ground state soliton and propagates for a long distance without distortion of its shape. Even if the initial pulse is in a parameter domain that is far from equilibrium, this pulse, still, will find its way (by either focusing or defocusing) to the ground state equilibrium exhibiting damped oscillations around it.

3. Spatiotemporal spinning solitons in pair plasmas

In this section we explore the possibility of the formation of spatiotemporal localized structures carrying a screw-type dislocation. Such structures in nonlinear optics are known as 'Spinning bullets' [14]. To establish the possibility of the

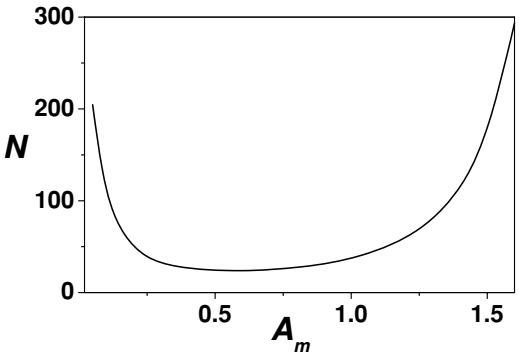

Figure 3. The dependence of the 'photon number' $N/10$ on the amplitude A_m.

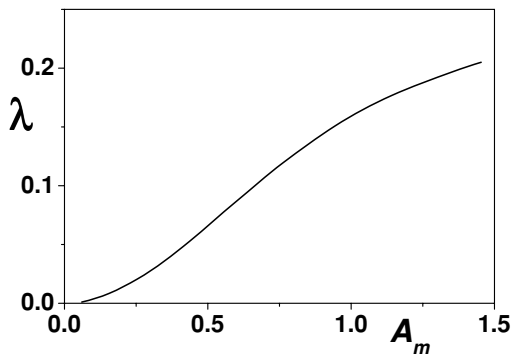

Figure 4. The effective Eigenvalue λ versus vortex amplitude A_m for $m=1$.

generation of stable spinning solitons in pair plasmas we first assume that the pulse is sufficiently long and effects related to the group velocity dispersion ($\sim \partial^2 A/\partial Z^2$) can be ignored.

Introducing polar coordinates (r, θ) to describe the(x, y) plane, we look for solutions of (1.3) in the form

$$A = A(r)\exp(i\lambda t + im\theta), \tag{3.1}$$

where the integer m defines the topological charge of the vortex and λ is the nonlinear frequency shift. The ansatz (3.1) converts (1.3) to the ordinary differential equation

$$\frac{d^2 A}{dr^2} + \frac{1}{r}\frac{dA}{dr} - \frac{m^2}{r^2}A - \lambda A + \frac{A^3}{(1+A^2)^2} = 0. \tag{3.2}$$

For non-zero m (the case of interest here), the ground state-localized vortex soliton has a positive amplitude, has a node at the origin $r=0$, reaches a maximum and then decreases monotonically as r increases. Such localized solution exists for $\lambda > 0$ and displays the following asymptotic behavior: $A_{r\to 0} \to r^{|m|}A_0$ and $A_{r\to\infty} \to \exp(-r\sqrt{\lambda})/\sqrt{r}$, where A_0 is a constant that measures the slope of A at the origin. Numerical simulations show that such localized solutions may exist in the range $0 < \lambda < \lambda_{cr} \approx 0.2162$ while the mode amplitude is a growing function of λ. Such behavior, calculated numerically, is presented in Fig. 4. for singlly charged vortices ($m=1$). The soliton amplitude (A_m), bounded from above by the critical value

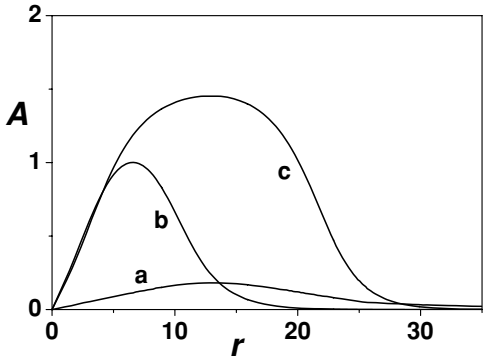

Figure 5. Profiles of solutions. Curves 'a', 'b' and 'c' correspond to $\lambda = 0.005; 0.16; 0.205$ respectively.

$A_{cr}(\approx 1.5)$, is found to be just moderately relativistic. Profiles of vortex solutions for different λs are illustrated in Fig. 5. One can again see that when pulse amplitude approaches the critical value, the profile settles into a flat-top shape. For the top part of such a solution (with $A(r) > 1$) the medium is defocusing while it tends to focus the lower intensity wings of the structure. Similar behavior of the solutions can be obtained for vortices with higher charge ($m = 2, 3, ...$); corresponding figures are not displayed here.

The intensity-dependent switching from the focusing to defocusing regime can have an interesting consequence for the stability properties of the solutions. The stability of vortex was conducted by following the linear stability procedure developed by [15], in which one considers perturbations acting along a ring of mean radius r_* , where $A(r_*) = A_m$. Assuming constant intensity and spatial uniformity for this ring, one can rewrite the diffraction operator in (1.3) as $\nabla_\perp^2 = r_*^{-2}\partial^2/\partial\theta^2$. The growth rate of the azimuthal perturbation with a phase factor $\Psi = \Omega t + M\theta$ (where M is an integer) then may be derived as

$$\mathrm{Im}(\Omega) = \frac{M}{r_*}\,\mathrm{Re}\left[\frac{2(1 - A_m^2)}{(1 + A_m^2)^3} - \frac{M^2}{r_*^2}\right]. \tag{3.3}$$

with the implication that large amplitude vortices with $A_m > 1$ are always stable. Lower amplitude vortex soliton, on the other hand, should decay into $M_{\max}$ multiple filaments, where $M_{\max}$ is an integer close to the number for which growth rate is maximal.

In Fig. 6 we plot $\mathrm{Im}(\Omega)$ versus M for $\lambda = 0.1$ and for $m = 1, 2$ and 3. The corresponding A_m are respectively 0.66, 0.65, 0.63, and $r_* = 6.3, 11.6, 16.9$ respectively. One should expect that instability will split the pulse into filaments (fragments) with number of filaments being respectively 2, 4 and 5 (or 6) for $m = 1, 2, 3$. These filaments must conserve total angular momentum. Since fusion of filaments is forbidden for topological reasons, they can eventually spiral about each other or fly off tangentially to the initial ring generating bright solitonic structures found, for instance, for the index saturation nonlinearity [14].

Numerical simulations for $A_m < 1$ give evidence of a quickly developing instability in agreement with predictions of the linear stability analysis. Indeed, we learn from Fig. 7 that the vortex soliton with $m = 1$ ($m = 2$) breaks up into 2 (4) filaments.

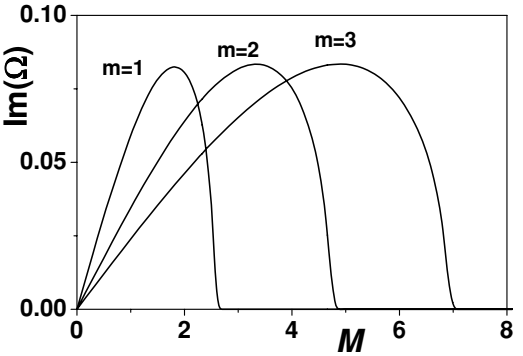

Figure 6. Instability growth rate $Im(\Omega)$ versus M for $\lambda = 0.1$ for different topological charges m.

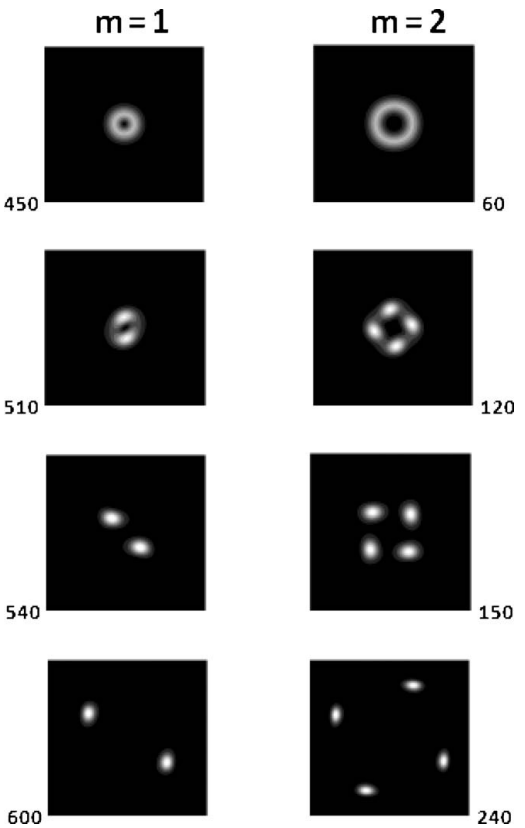

Figure 7. Vortex dynamics (for different time moments) when $\lambda = 0.1$: the left panel – for $m = 1, A_{max} = 0.66$, the vortex splits into two filaments; the right panel – for $m = 2, A_{max} = 0.6580$, the vortex splits into four filaments; the filaments are running away tangentially.

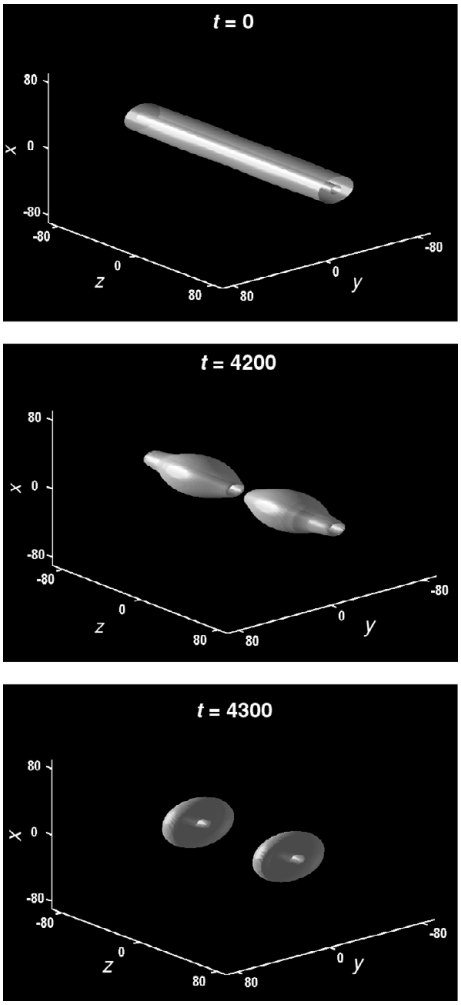

Figure 8. The breakup dynamics for the input vortex soliton with $m = 1$ and $A_m = 1.38$. Intensity donat-shape contours at $t = 4300$ correspond to the spinning bullets.

The filaments are running away tangentially without spiraling. All filament-like spatial solitons remain stable. Most interesting is the situation when amplitude of vortex soliton is larger than the unity. Long-time simulations for $A_m > 1$ have been conducted for the same m numbers. Simulations confirm the expectations of the linear stability analysis that the vortices maintain their fidelity and no breaking takes place; such vortices are exceptionally stable.

The inclusion of the effects related to the group velocity dispersion ignored up to now (term $\sim \partial^2 A/\partial Z^2$ in (1.3)) should have crucial importance in the dynamics of the process. It can lead to vortex soliton breaking along the propagation direction just as an ordinary self-trapped beam breaks into a train of spatiotemporal solitons – the 'light bullets' [16] – under the influence of a weak modulation instability. Similarly, we expect that longitudinal instability of 2D vortex soliton

and reshaping of the profile along the propagation direction could result in the generation of spatiotemporal bullets – 'Spinning bullets'.

This conjecture was verified by numerical simulations, in which the initial pulse was chosen to be a 2D vortex soliton with amplitude $A_m > 1$. The breaking up of the vortex beam into a chain of stable spatiotemporal pulses is illustrated in Fig. 8. Note that the zero vortex line survive structural changes.

4. Conclusions

The asymmetries originating in small temperature differences in the constituent species of an electromagnetically active medium may be always available for structure formation both in laboratory and cosmic/astrophysical settings. In the present paper we have shown that this asymmetry, mother to a new type of nonlinearity (derived in [12]), imparts specific properties to the sustained structures. We found that the pair plasmas, through the new focusing–defocusing nonlinearity generated by an 'asymmetry' in initial temperatures, can support multidimensional stable large amplitude light bullets as well as bullets carrying vortices, *i.e.* spinning bullets. Localized structures for certain parameters may have flat-top shapes. An investigation of such a nonlinearity is likely to advance our understanding of many naturally occuring physical systems, and one hopes that a focusing–defocusing nonlinearity can be created in the laboratory setting.

Acknowledgements

Authors express their thanks to Drs. S. I. Mikeladze and K. I. Sigua for their interest. Authors acknowledge special debt to the Abdus Salam International Centre for Theoretical Physics, Trieste, Italy. The work of SMM was supported by US-DOE Contract No. DE–FG 03-96ER-54366. The work of NLS and VIB was supported by ISTC Project G-1366 and Georgian NSF grant project GNSF 195/07 (GNSF/ST07/4-191).

References

[1] Wineberg, S. 1972 *Gravitation and Cosmology: Principles and Applications of the General Theory of Relatvity*. John Wiley and Sons, Inc. New York.

[2] Rees, M. J. and Mészáros, P. 1992 *MNRAS* **258**, 41; Mészáros, P. and Rees, M. J. 1993 *ApJ* **405**, 278; Mészáros, P. and Rees, M. J. 1993 *ApJ.* **418**, L5; Sari, R. and Piran, T. 1097 *ApJ* **485**, 270.

[3] Begelman, M. C., Blandford, R. D. and Rees, M. J. 1984 *Rev. Mod. Phys.* **56**, 255.

[4] Sturrock, P. A. 1971 *Astrophys. J.* **164**, 529; Ruderman, M. A. and Sutherland, P. G. 1995 *Astrophys. J.* **196**, 51; Michel, F. C. 1991 *Theory of Neutron Star Magnetospheres*. Chicago, IL: University of Chicago Press.

[5] Berezhiani, V. I., Tskhakaya, D. D. and Shukla, P. K. 1992 *Phys. Rev.* A**46**, 6608; Berezhiani, V. I., Garuchava, D. P. and Shukla, P. K. 2007 *Phys. Lett.* A **360**, 624; Chen, H. et al. 2009 *Phys. Rev. Lett.* **102**, 105001.

[6] Oohara, W. and Hatakeyama, R. 2003 *Phys. Rev. Lett.* **91**, 205005; Oohara, W., Date, D. and Hatakeyama, R. 2005 *Phys. Rev. Lett.* **95**, 175003.

[7] Oohara, W., Kuwabara, Y. and Hatakeyama, R. 2007 *Phys. Rev.* E **75**, 056403.

[8] Oohara, W. and Hatakeyama, R. 2007 *Phys. Plasmas* **14**, 055704.

[9] Shukla, P. K., Rao, N. N., Yu, M. Y. and Tsintsadze, N. L. 1986 *Phys. Reports* **31**, 1; Cattaert, T., Kourakis, I. and Shukla, P. K. 2005 *Phys. Plasmas* **12**, 012310; Shukla, P. K. and Khan, M. 2005 *Phys. Plasmas* **2**, 014504; Eliasson, B. and Shukla, P. K. 2005 *Phys. Rev.* E **71**, 046402; Tatsuno, T., Ohhashi, M., Berezhiani, V. I. and Mikeladze, S. V. 2007 *Phys. Letters* A **363**, 225; Berezhiani, V. I., Mahajan, S. M., Yoshida, Z. and Ohhashi, M. 2002 *Phys. Rev.* E **65**, 047402.

[10] Sabry, R., Moslem, W. M. and Shukla, P. K. 2009 *Phys. Plasmas* **16**, 032302; Berezhiani, V. I. and Mahajan, S. M. 1994 *Phys. Rev. Lett.* **73**, 1110; Berezhiani, V. I. and Mahajan, S. M. 1995 *Phys. Rev.* E **52**, 1968; Mahajan, S. M. and Shatashvili, N. L. 2008 *Phys. Plasmas* **15**, 100701; Esfandyari-Kalejahi, A., Kourakis, I., Mehdipoor, M. and Shukla, P. K. 2006 *J. Phys. A: Math. Gen.* **39**, 13817; Shatashvili, N. L., Javakhishvili, J. I. and Kaya, H. 1997 *Astrophys. Space Sci.* **250**, 109; Shatashvili, N. L. and Rao, N. 1999 *Phys. Plasmas* **6**, 66.

[11] Hatakeyama, R. 2008 Private communication.

[12] Mahajan, S. M., Shatashvili, N. L. and Berezhiani, V. I. 2009 *Phys. Rev.* E **80**(6), 066404; ArXiv:0909.0587 [physics.plasma-ph].

[13] Vakhitov, N. G. and Kolokolov, A. A. 1973 *Izv. Vyssh. Uchebn. Zaved. Radiofiz.* **16**, 1020 [Sov. Radiophys. **9**, 262]; Skarka, V., Berezhiani, V. I. and Miklaszewki, R. 1997 *Phys. Rev.* E **56**, 1080.

[14] Desyatnikov, A., Torner, L. and Kivshar, Y. S. 2005 *Prog. in Opt.* **47**, 291.

[15] Atai, J., Chen, Y. and Soto-Crespo, J. M. 1994 *Phys. Rev.* A **49**, R3170.

[16] Akhmediev, N. A. and Soto-Crespo, J. M. 1993 *Phys. Rev.* A **47**, 1358; Mahajan, S. M., Berezhiani, V. I. and Miklaszewki, R. 1998 *Phys. Plasmas.* **5**, 3264; Shukla, P. K., Marklund, M. and Eliasson, B. 2004 *Phys. Lett.* A **324**, 193.